CS-214

Centrifuge Model Tests on DMM Self Supported Wall in Soft Clay:

Tokyo Institute of Technology	Member, JSCE	Jiro Takemura
Tokyo Institute of Technology	Student member, JSCE	Ala'a El Nahas
Railway Research Institute	Member, JSCE	Masayuki Koda

Introduction: Four centrifuge experiments were conducted to study failure mechanism and pre-failure behavior of excavations supported by DMM self supported walls. In this paper, effects of the wall dimensions and the surface roughness on the stability during excavation were investigated.

Model Setup and Test Conditions: Figure 1 shows the test setup. Its main components are steel box, model DMM wall, in-flight excavator, soil retaining gate and sensors. Table 1 shows the test condition and the excavation heights at failure, $(z_e)_f$. Height, width and surface conditions of the wall are the parameters varied in the tests. The box is connected to a drainage tank. The model wall is consisted of aluminum and acrylic plates. Earth pressure cells were instrumented on the front and back surfaces of the wall as well as its bottom. Rough wall surface condition was made by pasting sandpaper on the wall surfaces. Centrifugal acceleration used was 70g.

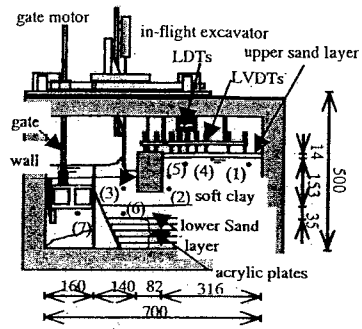

Figure 1 Test Setup

Model ground: Soil layers in the model are an upper dry loose Toyoura sand, a soft kaolin clay, and a lower dense Toyoura sand, as shown in Figure 1. Thickness of these layers were 14mm, 153mm and 35mm, respectively. The wall was floated in the clay not founded on the lower sand in all tests. Physical and mechanical properties of the kaolin clay are shown in Table 1. Figure 2 shows the clay water content and undrained strength profiles. The water content was measured after the test, and the undrained strength was calculated from the average water content values.

Table 1 Test condition:

Test No.	Surface condition	H (mm)	B (mm)	H/B	$(Z_e)_f$ (mm)
SSW-0	Smooth	123	82	1.50	32
SSW-3	Rough	123	82	1.50	43
SSW-4	Rough	163	82	1.99	64
SSW-5	Rough	123	123	1.00	67

H & B are the wall height and width

Table 2 Main physical and mechanical properties of the kaolin clay:

Liquid limit,(%)	Plastic limit,(%)	G_s	c_u/p' (N.C. clay)
77.5	30.3	2.61	0.24

Excavation Procedure: Excavation was conducted step by step using in-flight excavator as shown in Figure 1. In each step, soil was cut by 10 mm height from the front of the wall. The water level in the excavated area was lowered by draining water from the box to the drainage tank, so that it became the same as the excavation bottom. Excavation process with time is shown in prototype scale in Figure 3. Details of the test procedures are given elsewhere [1].

Test Results and Discussion: Figure 4 shows the soil and wall displacements observed in SSW-0/3/4. Marked horizontal displacement and less vertical one was observed in the wall, which clearly shows sliding type failure. On the active sides, the failed zones were bounded with a clear failure plane. The failure plane in SSW-0 with smooth surface is steeper than those in SSW-3/4 with rough surface, resulting in wider failure zone in the latter than the former. The soil outside these planes and below the wall didn't show any remarkable strain even after failure. On the passive sides, the soil deformed laterally with some vertical heave, without showing any clear failure planes.

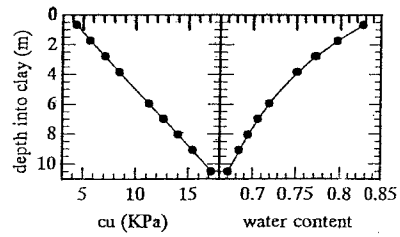

Figure 2 Clay strength and water content profiles

Figure 5 shows the horizontal displacements of the wall bottom, dh, during excavation. Until some depth of excavation, only very small displacement was observed and then a sudden increase took place without showing gradual increase. From this figure failure excavation heights, $(z_e)_f$, was defined as the excavation height at the intersection of the tangents for the z_e-dh relationships before and after sudden increase. Failure height of each test is pointed with an arrow in the figure. It can be clearly seen from SSW-0 and 3 that roughness or adhesion on the wall surface contribute the increase of wall stability.

Figure 6 shows the variation of maximum settlement, S_{max}, of the retained soil behind the wall during excavation. S_{max} was small before the failure, and increased sharply at the failure point just like dh shown in Figure 5. This trend is more apparent in SSW-0/3. However, in SSW-4/5, the transition from the initial tangent to the failure

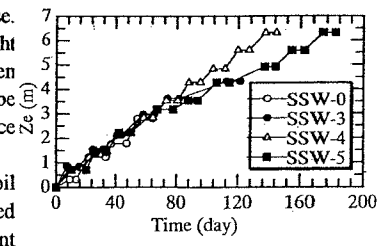

Figure 3 Excavation progress

Key words: DMM,soft clay, excavation, failure, earth pressure, and displacement
Address: Civil Engineering Department, Tokyo Institute of Technology, 2-12-1 O-okayama, Meguro-ku, Tokyo 152-855.

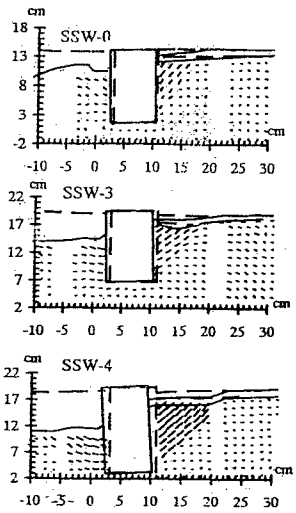

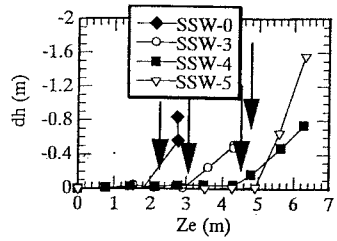

Figure 5 Wall base horizontal displacements

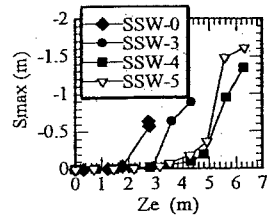

Figure 6 S_{max}-Z_e relationships

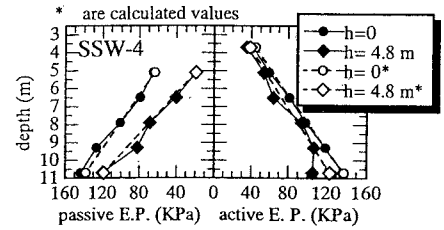

Figure 7 Measured and calculated active and passive earth pressures

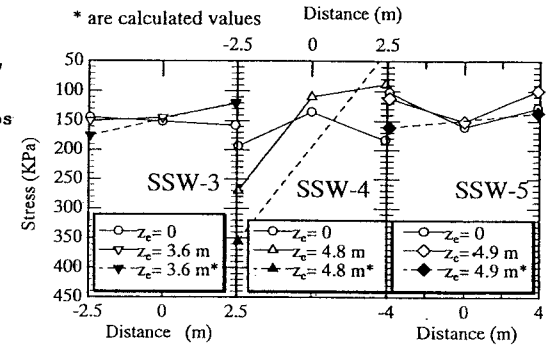

Figure 8 Measured and calculated bearing stresses under the wall

was relatively gradual. For SSW-4/5, $(z_e)_f$ was nearly similar (4.5 m and 4.7 m). Thus, increasing B by 50% resulted in almost the same increase in $(z_e)_f$ obtained by increasing H by 30 %. Therefore, for the wall floating in NC clay of which strength increasing with depth, increasing the wall length is more effective than its breadth in increasing the failure excavation height.

Figure 7 shows the measured and calculated active and passive earth pressure distributions on the wall in SSW-4 before excavation and just after failure. The predicted values after failure were calculated by the following equation proposed by Rowe [2].

$$p(z)_{a,p} = \gamma z + p \mp 2c_u(z)\sqrt{1 + c_w / c_u(z)}$$

where c_w is the adhesion between the wall and surrounding clay and p is surcharge. c_w/c_u= 0.6 was assumed in the calculation. The predicted values agreed with the measured values. The differences between the active and the at-rest earth pressure distributions are small. That is referred to the low shear strength of the soft clay soil. Therefore, the major constituent of the active and passive earth pressures was the vertical pressure due to the soil own weight.

Figure 8 shows the measured and calculated contact pressures on the wall base before excavation and just after failure for SSW-3/4/5. The calculated values were determined using a classic external stability analysis used in the design of the gravity type walls [3]. Although some scattering was observed before excavation, it can be clearly seen that variations of contact pressure were very small from the initial to the failure in SSW-3(H/B=3/2) and 5(H/B=1). While for SSW-4 with rather small H/B (=2), quite large increase and decrease of the contact pressures were at the front and back toes of the wall base, but the contact pressure distribution was more uniform than the calculation. These imply that tilting failure may possibly dominate for the wall with H/B larger than 1/2. Although increasing H is much more effective in increasing $(z_e)_f$, it should be noted that increasing H also increases the eccentricity of the bearing stresses on the soil under the wall.

Conclusions:

1. For H/B= 1~2: failure mechanism for excavations supported by this wall type is sliding.
2. Increasing the wall length rather than its width is much more effective in increasing its stability especially for the NC clay of which strength increases with depth. However, increasing the length is accompanied by higher eccentricities for the wall bearing stresses on the underlying soil.

References:

1. El Nahas, A., et al., (1999). "Stability of excavations in soft clay supported by DMM self supported walls", IS-Tokyo 99, (to appear)
2. Rowe, P.W. (1957). "Sheet pile walls in clay", Instn. Civ. Engrgs, Vol. 7, July, pp. 629-654.
3. Shiomi, et al., (1996). "Slope stability using the admixture method", Proc. IS-Tokyo 96, Grouting and Deep Mixing, pp. 563-568.